RESEARCH ARTICLE

Key Points:
- Deep ventilation occurs regularly in the Red Sea
- Dense water is produced in the northern Red Sea with Suez and Aqaba Gulfs included
- Water circulation modulates the surface cooling

Correspondence to:
V. P. Papadopoulos,
vassilis@hcmr.gr

Factors governing the deep ventilation of the Red Sea

Vassilis P. Papadopoulos[1], Peng Zhan[2], Sarantis S. Sofianos[3], Dionysios E. Raitsos[4], Mohammed Qurban[5], Yasser Abualnaja[6], Amy Bower[7], Harilaos Kontoyiannis[1], Alexandra Pavlidou[1], T. T. Mohamed Asharaf[5], Nikolaos Zarokanellos[6], and Ibrahim Hoteit[2]

[1]Hellenic Centre for Marine Research, Anavissos, Greece, [2]Physical Science and Engineering Division, KAUST, Thuwal, Saudi Arabia, [3]Department of Physics, University of Athens, Greece, [4]Plymouth Marine Laboratory, Plymouth, UK, [5]King Fahd University of Petroleum and Minerals, Dhahran, Saudi Arabia, [6]Red Sea Research Centre, KAUST, Thuwal, Saudi Arabia, [7]Woods Hole Oceanographic Institution, Woods Hole, Massachusetts, USA

Abstract A variety of data based on hydrographic measurements, satellite observations, reanalysis databases, and meteorological observations are used to explore the interannual variability and factors governing the deep water formation in the northern Red Sea. Historical and recent hydrographic data consistently indicate that the ventilation of the near-bottom layer in the Red Sea is a robust feature of the thermohaline circulation. Dense water capable to reach the bottom layers of the Red Sea can be regularly produced mostly inside the Gulfs of Aqaba and Suez. Occasionally, during colder than usual winters, deep water formation may also take place over coastal areas in the northernmost end of the open Red Sea just outside the Gulfs of Aqaba and Suez. However, the origin as well as the amount of deep waters exhibit considerable interannual variability depending not only on atmospheric forcing but also on the water circulation over the northern Red Sea. Analysis of several recent winters shows that the strength of the cyclonic gyre prevailing in the northernmost part of the basin can effectively influence the sea surface temperature (SST) and intensify or moderate the winter surface cooling. Upwelling associated with periods of persistent gyre circulation lowers the SST over the northernmost part of the Red Sea and can produce colder than normal winter SST even without extreme heat loss by the sea surface. In addition, the occasional persistence of the cyclonic gyre feeds the surface layers of the northern Red Sea with nutrients, considerably increasing the phytoplankton biomass.

1. Introduction

Deep water renewal is vital for the marine ecosystems throughout the global ocean. Rich in atmospheric oxygen, waters from the sea surface can reach the bottom after becoming dense enough to penetrate the underlying layers. The so-generated thermohaline circulation fuels the overturning oceanic conveyor belt, redistributes the heat, and recycles oxygen and nutrients in the ocean. The sustainability of the global overturning circulation is a fundamental factor for the earth's climatic stability. Like the global ocean, marginal seas also rely on the thermohaline circulation for their deep water renewal. Especially for oligotrophic marine ecosystems like the one of the northern Red Sea [*Acker et al.*, 2008; *Labiosa et al.*, 2003; *Raitsos et al.*, 2013], deep mixing has a twofold effect intimately associated with the basin ecosystem functioning. It ventilates the near-bottom layer and transfers significant amounts of nutrients from deeper layers to the nutrient-depleted surface, resulting in a significant increase in phytoplankton biomass (the foundation of the marine food chain). Concurrently, dense water formation is of great importance for the regional climate as it reflects the response of the surface waters to the winter atmospheric forcing.

The elongated Red Sea basin (Figure 1) is a typical example of a semienclosed marginal sea which exchanges water with the Indian Ocean. Water with relative low salinity enters the basin in a surface layer through the strait of Bab El Mandeb at its southern end, while saltier water flows out underneath to the Gulf of Aden [*Murray and Johns*, 1997; *Matt and Johns*, 2007; *Johns and Sofianos*, 2012; *Churchill et al.*, 2014; *Yao et al.*, 2014a,b]. As evaporation exceeds by far precipitation throughout the Red Sea, the northward flowing fresher water becomes gradually saltier with salinity higher than 40 to the far north [*Morcos*, 1970; *Woelk and Quadfasel*, 1996; *Plähn et al.*, 2002; *Sofianos and Johns*, 2007]. It is in the far north, mostly inside the gulfs of Aqaba (Eilat) and Suez, where the hypersaline surface water experiences the winter atmospheric forcing
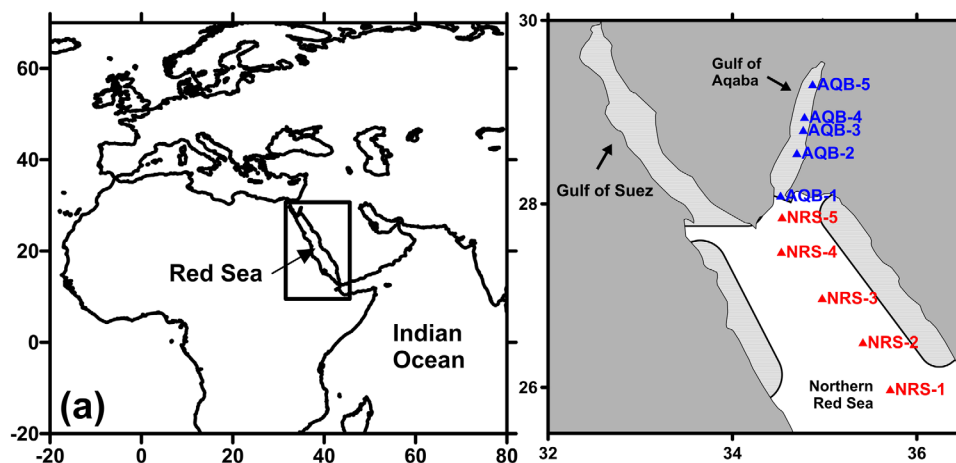
Figure 1. The location of the Red Sea, the line of hydrographic stations repeatedly carried out in November 2013 and March 2015, and the areas of spatially averaged MODIS SST (shadowed). Stations NRS-4, NRS-3, and NRS-2 coincide with stations carried out during KAUST 2010 and 2011, and KFUPM 2012 expeditions.

[*Woelk and Quadfasel*, 1996; *Sofianos and Johns*, 2003; *Biton and Gildor*, 2011a,b; *Papadopoulos et al.*, 2013, *Abualnaja et al.*, 2015] and becomes cold and dense enough to sink, reaching intermediate and near-bottom layers.

Intermediate water is believed to form regularly every winter over the open northern Red Sea and travels back to the south. This water flows out to the Gulf of Aden and to the Indian Ocean as the Red Sea Outflow Water (RSOW), the main subsurface branch of the Red Sea overturning circulation [*Eshel et al.*, 1994; *Eshel and Naik*, 1997; *Sofianos and Johns*, 2003, 2007; *Yao et al.*, 2014a,b]. Below the intermediate water lies the Red Sea deep water which occupies the most of the water column from about 200 m to the bottom throughout the basin [*Sofianos and Johns*, 2007].

The mechanism of the deep water formation has been a controversial issue for more than half a century. Thus far, several theories have been introduced based on scarce direct hydrographic data or using tracers to locate the source of the deep waters. It is most likely that dense water, with the potential to renew and ventilate the near-bottom layers of the Red Sea, can be produced only within the Gulfs of Aqaba and Suez at the northernmost edge of the basin during winter [*Wyrtki*, 1974; *Cember*, 1988; *Woelk and Quadfasel*, 1996; *Clifford et al.*, 1997; *Plähn et al.*, 2002; *Manasrah et al.*, 2004; *Biton and Gildor*, 2011a]. However, direct observations required to describe in detail the mechanism of deep water formation in the northern basin are still factually missing.

The current study employs a wide range of observations and reanalysis data to highlight the regularity of the deep ventilation of the Red Sea and address factors affecting the interannual variability of the deep water renewal. We identify potential origins and pathways of the densest Red Sea waters and address factors that regulate substantially the amount of deep water produced every winter in the northern Red Sea. The manuscript is organized as follows. Section 2 refers to data employed in the study and the methodology adopted. Section 3 provides evidence of regular dense water formation over the northern Red Sea. In section 4, several winter events are analyzed, while section 5 outlines factors with the potential to modulate the deep water formation. Section 6 provides a summary of the results emerging from the study and addresses issues that remain unresolved.

2. Data and Methods

2.1. The Data Sets

Hydrographic data used in this study come from six recent cruises carried out by the Greek Research Vessel AEGAEO in the Red Sea in March 2010, September 2011, November 2012, November 2013, March 2013, and March 2015. These cruises were conducted by the Saudi Arabian Universities, King Abdullah University of Science and Technology (KAUST) and King Fahd University of Petroleum and Minerals (KFUPM). We also

refer to hydrographic data collected during several historic oceanographic cruises in the Red Sea [*Morcos*, 1970; *Morcos and Soliman*, 1974; *Wyrtki*, 1974; *Cember*, 1988; *Woelk and Quadfasel*, 1996; *Manasrah et al.*, 2004; *Sofianos and Johns*, 2007].

Monthly mean air-sea net heat flux is calculated by summing the four flux components as retrieved by the NASA Modern Era Retrospective-Analysis for Research and Applications (MERRA) [*Rienecker et al.*, 2011]. In addition, monthly mean turbulent air-sea heat fluxes (the sum of latent and sensible heat) obtained from WHOI OAFlux archive [*Yu et al.*, 2008] are complementarily employed. Sea level anomalies (SLA) used in this study are data merged from the TOPEX/POSEIDON, GFO (Geosat Follow-On), Jason-1, Envisat, and ERS satellites provided by AVISO (ftp://ftp.aviso.oceanobs.com/global/dt/upd/msla/merged/) on a regular 0.25° grid every 7 days from October 1992 to December 2012. The merged product combines data from different missions and has fewer mapping errors and better spatial coverage than products based on one satellite alone [*Ducet et al.*, 2000]. Large-scale surface air temperature employed in the study is obtained from ERA-Interim Reanalysis [*Dee et al.*, 2011]. We also use time series of surface air temperature from a meteorological station located at the northern edge of the Gulf of Aqaba (Eilat). Data recorded by this station are freely available at http://www.iuieilat.ac.il/Research/NMPMeteoData.aspx.

The weekly (8 day composites) satellite remotely sensed ocean color (Chl *a*) and SST data set were acquired from NASA's Oceancolor web base (http://oceancolor. gsfc.nasa.gov). The Moderate-resolution Imaging Spectroradiometer (MODIS on board the Aqua platform) 4 km resolution data sets were processed for the period 2002–2014. To avoid the solar radiation bias in the remotely sensed SST observations, which occurs during the day-time (from surface heating), only the nighttime product was acquired. Satellite SST observations have been used before in the Red Sea to investigate seasonal and interannual variability, and more detailed data description could be found elsewhere [*Raitsos et al.*, 2011].

Regarding the near-surface Chl *a* estimates, the standard NASA algorithm (OC3) was used, that is routinely processed by the Ocean Biology Processing Group at the Goddard Space Flight Center [*Feldman and McClain*, 2012]. Satellite-derived Chl *a* data have known limitations especially in optically complex waters, where particulate and/or dissolved organic matter do not covary in a predictable manner with Chl *a* [*Morel and Gentili*, 2009]. Therefore, Chl *a* data may be influenced (generally resulting in an overestimation) by the factors mentioned above, especially in the coastal waters and/or very shallow waters of the Red Sea (such as coral reefs). A small portion of our study area includes such optically complex waters. However, the potential overestimation of Chl *a* in such areas does not mean that all the coastal high chlorophyll values are necessarily erroneous. For instance, large coral reef complexes may be sources of either nutrients or chlorophyll-rich detritus that enhance phytoplankton production near the reefs [*Acker et al.*, 2008]. In fact, recent evidence clearly shows a highly significant relationship between satellite and in situ Chl *a* at coral reef areas of the Red Sea [*Racault et al.*, 2015], including our study area. In addition, a reasonable agreement between satellite-derived Chl *a* and in situ LiDAR fluorescence-derived Chl *a* has been shown in the Red Sea [*Barbini et al.*, 2004]. Furthermore, a recent comparison between MODIS Chl *a* and in vivo fluorometric Chl *a* measurements collected over large spatial scales clearly indicated that the performance of the standard NASA chlorophyll algorithm is found to be comparable with other oligotrophic regions in the global ocean, supporting the use of satellite ocean color in the Red Sea [*Brewin et al.*, 2013].

2.2. Methodology

The main goal of this study is to explore the factors affecting the water renewal of the near-bottom layer in the Red Sea. The dissolved oxygen (hereafter DO) concentration is a fundamental indicator to identify new dense water formation. DO measurements, obtained by a CTD profiler (SBE-19 model) and calibrated against sea water sampling [*Carpenter*, 1965], are used to trace the ventilation of the water column and particularly the renewal of the near-bottom layers. As the deep ventilation is intimately dependent on the surface water cooling, SST satellite observations are employed to show year-to-year winter SST characteristics and to detect the potential origin of the Red Sea deep water. Furthermore, SST is used to trace upwelling events over the northern Red Sea and their possible relation to dense water formation. Upwelling events are also related with cyclonic eddies and we use satellite observations of SSH to explore the surface circulation over the northern Red Sea. Since the surface phytoplankton blooms in the northern Red Sea are dependent on nutrients emerging from deeper layers [*Raitsos et al.*, 2013; *Triantafyllou et al.*, 2014], temporal variation of Chl *a* is also analyzed to describe the intensity of upwelling events. Finally, the atmospheric forcing over the northern Red Sea
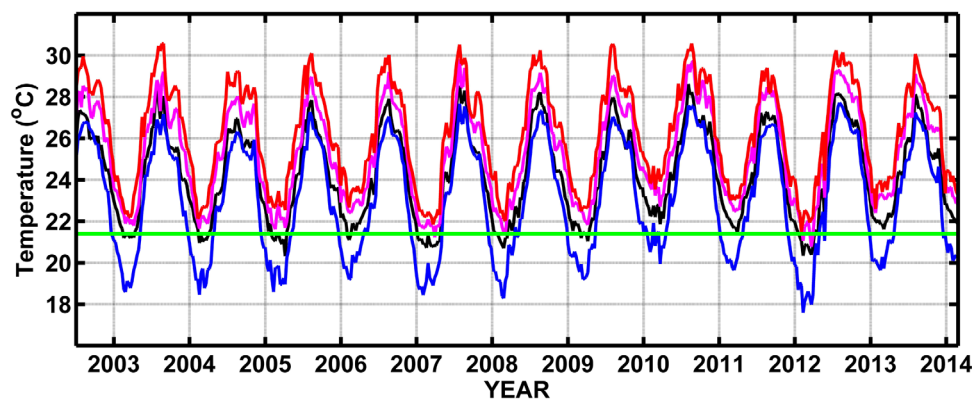
Figure 2. MODIS SST spatially averaged time series for the Gulf of Aqaba (black line), the southern part of the Gulf of Suez (blue), the western part of the northern Red Sea (magenta), and the eastern part of the northern Red Sea (red). The green line depicts the Red Sea deep water potential temperature.

is examined using reanalysis data for air-sea heat exchange and surface air temperature, and air temperature from a meteo station located at Eilat (northernmost edge of the Gulf of Aqaba).

3. The Regularity of the Deep Water Formation

Historical oceanographic cruises in the Red Sea, though rare, started in 1935. Hydrographic data collected thus far consistently show that the near-bottom layer is more oxygenated than the overlying layers everywhere in the basin [*Morcos*, 1970; *Morcos and Soliman*, 1974; *Wyrtki*, 1974; *Cember*, 1988; *Woelk and Quadfasel*, 1996; *Sofianos and Johns*, 2007]. This pattern indicates that deep water formation takes place over the northern part of the basin and sustains the ventilation of the deep Red Sea layers on a long-term basis. However, the ventilation events may show strong interannual variability in the origin and the amount of the deep water. CTD casts carried out during the recent KAUST and KFUPM expeditions suggest that the potential temperature of the deep waters in the Red Sea is considerably steady. Sea water below 500 m is characterized by potential temperature between 21.40°C and 21.50°C. This range narrows for the water column below the depth of 1000 m where potential temperatures are between 21.40°C and 21.45°C. At the same time, salinity below 250–300 m is constantly greater than 40.50 and ranges between 40.55 and 40.57 at depths greater than 1000 m throughout the Red Sea. As the potential temperature is a conservative property of the sea water, any surface water that obtains a temperature less than 21.40°C has the potential to reach the bottom layer provided that an appropriate salinity coexists. In fact, due to entrainment of warmer subsurface water during the sinking of the surface water, this temperature should be lower but still remains a practically absolute threshold for identifying areas of potential contribution to the deep water feeding.

Figure 2 shows composite (average values based on a number of grid points) satellite-derived SST time series representative for different areas (shadowed in Figure 1b) of the northern Red Sea for the period 2002–2014. During winter, the waters inside the Suez Gulf are by far the coldest waters in the region, reflecting the direct influence by air masses coming from higher latitudes and the limited water volume of the shallow gulf. The average SST of the Suez Gulf is colder than the theoretical threshold of 21.40°C for a considerable time every winter. At the same time, data obtained from the National Oceanographic Data Centre (NODC) and several cruises show that the salinity inside the gulf is the highest over the whole Red Sea with values 42–44 [*Sofianos and Johns*, 2015]. Thus, dense water of Suez origin is expected to contribute every year to the near-bottom ventilation of the Red Sea. Although several works attempted a volume estimation of the annual deep water formation [*Wyrtki*, 1974; *Mallard*, 1974; *Murray et al.*, 1984; *Biton and Gildor*, 2011a; *Sofianos and Johns*, 2015], the precise amount and the mechanism of the formation are still practically unknown.

The Gulf of Aqaba is the second coldest area among those considered in Figure 2. If we take into account that its northern part is characterized by even lower temperatures than the average presented here, and its higher salinity compared with the open Red Sea [*Morcos*, 1970; *Paldor and Anati*, 1979; *Plähn et al.*, 2002], the Gulf of Aqaba should be also considered as a regular supplier of Red Sea near-bottom waters. Figure 3 shows the profiles of the DO concentration from CTD casts carried out just inside and outside the Gulf of
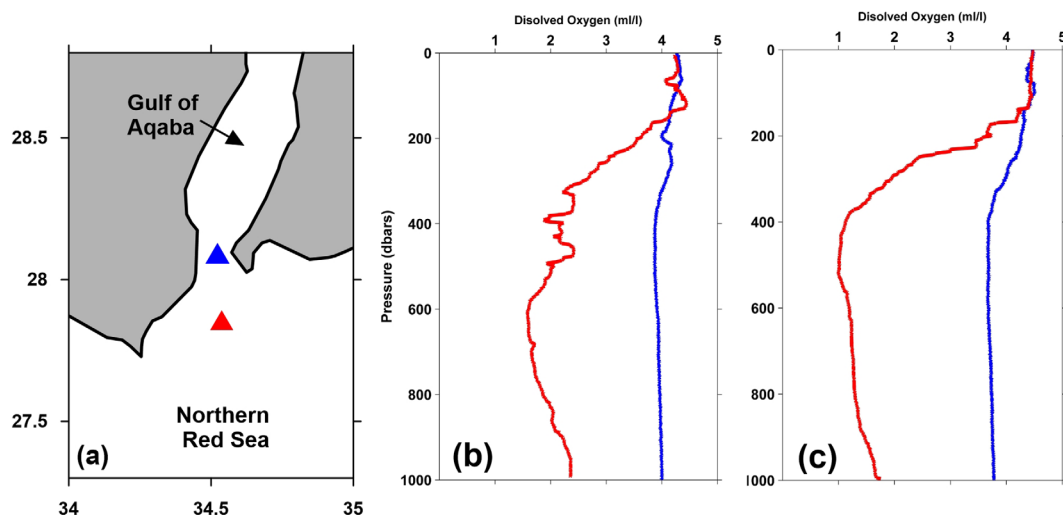
Figure 3. (a) Location of the two CTD stations carried out in November 2013 and March 2015 and the corresponding dissolved oxygen profiles (b) for 2013 and (c) for 2015 just inside (blue) and outside (red) the Gulf of Aqaba.

Aqaba during two recent oceanographic cruises (November 2013 and March 2015). The distance between the two stations is 14 nm with the sill (∼300 m according to a recent multibeam survey) of the Strait of Tiran between them (Figure 3a). Inside the Gulf, the whole column is characterized by water rich in DO with concentrations varying little with depth. It is noteworthy that surface waters in November 2013 (Figure 3b) contain only 0.2 mL/L more DO than those overlying the bottom. The difference in DO between surface and near-bottom water increases to 0.5 mL/L in March 2015 (Figure 3c). This implies active ventilation of the entire water column inside the gulf, yet presenting considerable temporal variability. Just a few miles outside the Aqaba Gulf, the DO profiles obtained in both cruises are dramatically different. The first 150 m of the water column are well oxygenated with values around 4 mL/L(DO saturation >90%). A progressive decrease of DO is observed reaching a minimum value of 0.9 mL/L (March 2015) and 1.5 mL/L (November 2013) at 600 m. Deeper than 600 m, the DO concentration increases again to reach slowly a secondary maximum of 1.75 mL/L (March 2015) and 2.3 mL/L (November 2013) just over the bottom. Although the open sea profile provides evidence of deep water oxygenation, the deep water, compared to that inside the Gulf, has a significantly reduced DO, revealing a limited volume of water outflow from the Aqaba Gulf. This is in agreement with several earlier studies [Cember, 1988; Plähn et al., 2002; Biton and Gildor, 2011a,b].

Water exchange between the Gulf of Aqaba and the open northern Red Sea takes place through a two-layered circulation with surface inflow of relatively fresher water and subsurface outflow of saltier water [Murray et al., 1984]. The water flowing from the Aqaba Gulf is denser than the open Red Sea water of the same depth as shown by potential density (sigma-theta) transects inside and outside the Gulf for the cruises conducted in 2013 and 2015 (Figure 4). This is in agreement with the results of the study carried out by Manasrah et al. [2004]. However, the density at the bottom of the sill exhibits significant temporal variability (Figure 4). The higher the density of the water flowing outside the gulf, the higher the possibility of that water to reach the near-bottom layer of the open Red Sea. As this dense water flows out from the Gulf of Aqaba, it sinks piercing the layer of minimum DO (500–600 m) observed in the open Red Sea, while its DO decreases considerably due to entrainment. Indeed, all of the DO profiles observed in the northern Red Sea (Figure 5) show an intermediate DO minimum at a depth around 500–600 m. This intermediate DO minimum indicates that dense water sinks to reach the bottom in the open northern basin laterally with the incoming water to be advected along the northern slope of the Red Sea. Again, this is in full agreement with the findings of previous studies [see Sofianos and Johns, 2007, Figure 5].

Average SST values representative of the western and eastern parts of the northernmost Red Sea (Figure 2) along with salinities observed over the northern Red Sea show that these two regions have the lowest possibility of producing water dense enough to reach the near-bottom layers. Nevertheless, water temperature and salinity found in the near-bottom layer of the Red Sea can be observed in the surface layers over the northern end of the open Red Sea. Several studies refer to salinities higher than 40 observed over the open
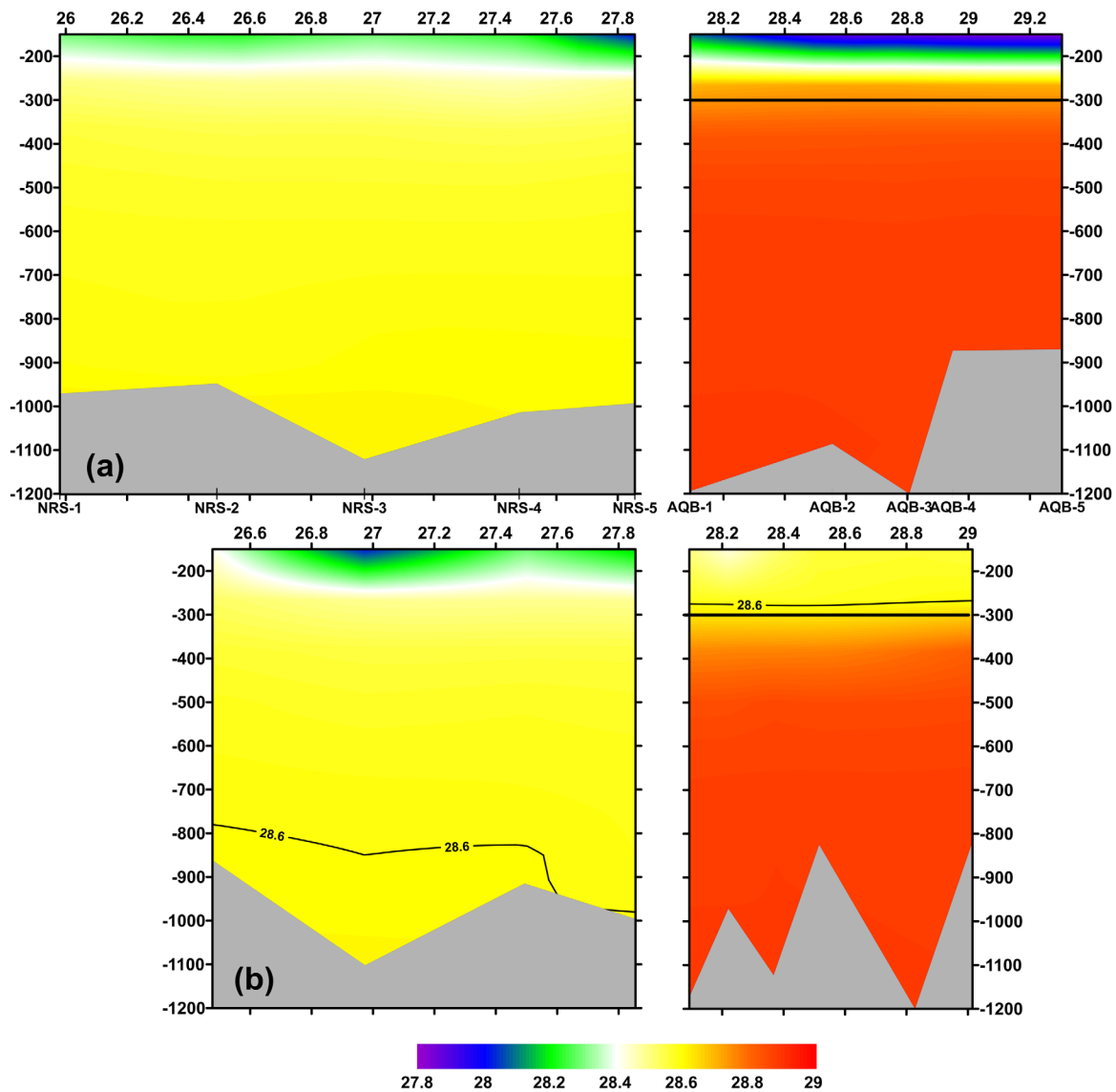
Figure 4. Potential density transects for the water column deeper than 150 dbars (db) in (left) the open northern Red Sea and (right) the Gulf of Aqaba from the cruises conducted by KFUPM in (a) November 2013 and (b) March 2015. The thick black line in the Aqaba Gulf section corresponds to the sill depth. The 28.6 isopycnal is plotted for a better discrimination of the density distribution in the sill depth and near-bottom layers inside and outside the gulf, respectively.

northern basin [*Morcos*, 1970; *Mallard and Soliman*, 1986; *Quadfasel and Baudner*, 1993; *Woelk and Quadfasel*, 1996; *Sofianos and Johns*, 2007]. Furthermore, in the frame of a long-term monitoring project over the northeastern part of the Red Sea conducted by KFUPM, salinity measurements consistently ranged between 40.6 and 42.1 at two different coastal sites in June 2011 and September 2012. Thus, it is quite possible that salinity values higher than 40.55 can be occasionally found in the northernmost coastal areas along with appropriate cold temperatures. In terms of temperature, several winters such as those of 2004, 2007, 2008, and especially that of 2012 show average SST very close or even lower than 21.4°C, mainly at the western part of the northern Red Sea. Therefore, it is plausible that dense water may originate from shallow coastal areas and from there, it sinks to reach the deep layers of the Red Sea.

4. Warm and Cold SST Events

The amount of water that ventilates every winter the near-bottom layers of the Red Sea is mostly expected to follow the intensity of the atmospheric forcing. The total contribution from the Gulfs of Suez and Aqaba
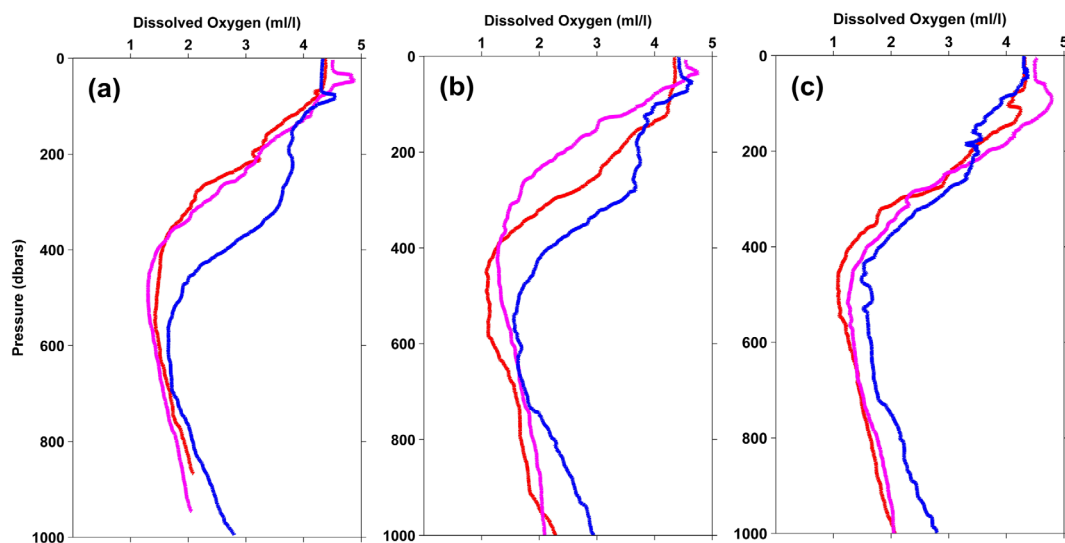
Figure 5. Dissolved oxygen profiles for the stations (a) NRS5, (b) NRS4, and (c) NRS3 obtained in March 2010 (red), October 2011 (magenta), and November 2012 (blue).

to the deep layers of the Red Sea is estimated between 0.05 and 0.1 Sv [*Sofianos and Johns*, 2015]. A question arising here is if there are additional factors favoring or impeding the dense water formation over the northernmost end of the Red Sea. Between the autumns of 2011 and 2012, a noticeable increase of DO in the bottom layers was observed over the northern part of the Red Sea (Figure 5). In February and March of 2013, during the KAUST 2013 Red Sea Expedition, a similar increase in the near-bottom DO was detected, even at the central part of the basin. Spatially averaged SST values representing the northern basin suggest that this increase in DO could be attributed to the onset of newly formed deep water resulted by the abnormal surface cooling during the winter of 2012. Indeed, the time plots of Figures 2 and 6a show that the winter of 2012 exhibits the coldest SST in the last 12 years 2003–2014 for all areas considered. The 2012 event also coincides with a significant increase in Chl *a* concentration over the northernmost part of the Red Sea (Figure 6b). This reflects to extensive transfer of nutrient-rich deep water to the surface layers. Since the surface cooling is typically linked to the observed net air-sea heat exchange (Q_{net}), the temporal variability of Q_{net} is of high interest. Figure 5c shows the winter mean Q_{net} derived by MERRA archive, spatially averaged to represent the open northernmost part of the Red Sea. The winter mean is the average of the monthly mean values for November, December, January, and February (NDJF). We select these four specific months because during NDJF the maximum heat loss is observed over the northern Red Sea. Interestingly, Q_{net} shows that the strongest heat loss from the sea surface occurred not in the winter of 2012 but in that of 2008. On the other hand, the mean Q_{net} of the warmest winter in 2010 is not the highest in the 12 years 2003–2014. In addition, this warmest winter is also associated with a minimum Chl *a* concentration indicating low nutrient availability due to limited vertical mixing. Indeed, the northern part of the Red Sea follows the typical plankton-climate link seen in the tropics, where stronger thermal stratification during warmer climate periods reduces vertical mixing (lowering the supply of nutrients from deeper waters), and limits phytoplankton growth [*Raitsos et al.*, 2015].

Examining carefully Figure 6, we observe that even in winters with commensurate SST minima like the ones that occurred in 2007 and 2008 (Figure 6a), the corresponding Q_{net} varies disproportionally (Figure 6c). As mentioned above, the winter of 2008 displays the strongest heat loss from the sea to atmosphere (lowest Q_{net}) indicating that during that winter the northern part of the Red Sea experienced the strongest atmospheric forcing. However, the lowest SST is observed during the winter of 2012. To compare the difference in the atmospheric forcing between those two winters, we show the winter (NDJF) mean anomaly of the air temperature over a broad area surrounding the Red Sea for both 2008 and 2012 (Figures 7a and 7b). Both exhibit negative air temperature anomalies over the northern half of the Red Sea and neighboring areas (Middle East, Arabian Peninsula, and Northern Africa), but the winter in 2008 was colder than the one in 2012, with a lower surface air temperature around 1°C on average. This is also inferred by the air
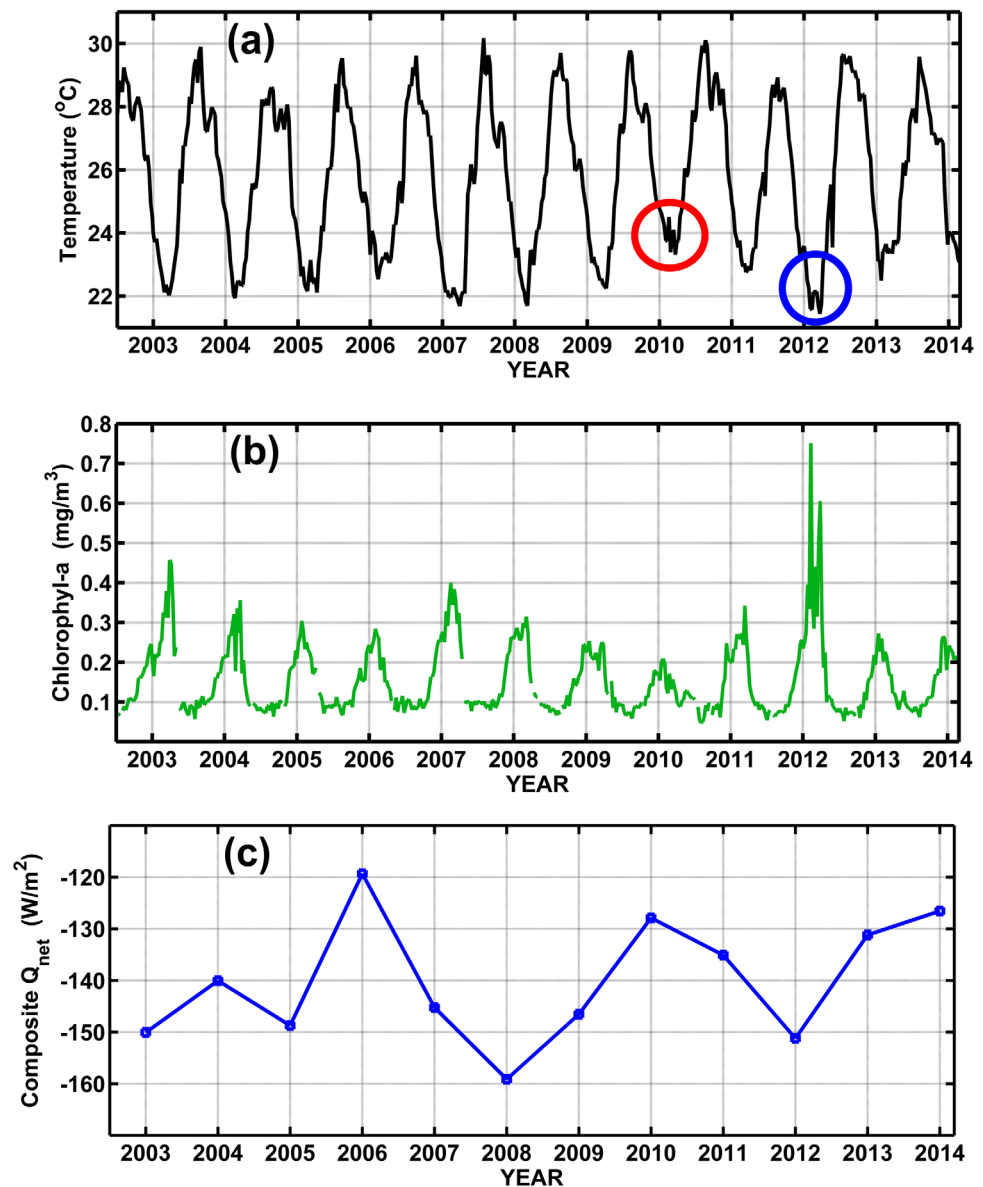
Figure 6. (a) Composite MODIS SST time series for the open northern Red Sea with the warmest (red) and the coldest (blue) winter observed during the 12 years 2002–2014; (b) as in Figure 6a but for the chlorophyll *a*; (c) winter (NDJF) mean Q$_{net}$ averaged for the open northern Red Sea.

temperature recorded in Eilat (northernmost edge of the Gulf of Aqaba, Figure 7c). In terms of air-sea heat flux, turbulent components are the fundamental factor regulating the sea surface cooling. Radiative terms are much more stable than turbulent terms and contribute only by a small fraction to the air-sea heat flux variability over the northern Red Sea [*Papadopoulos et al.*, 2013]. In accordance to Q$_{net}$ and to air temperature, OAFlux turbulent components show a weaker surface heat loss during the winter of 2012 than in that of 2008 (not shown). Figures 6a and 6b also suggest that winters of similar SST are associated with dissimilar Chl *a* concentrations. This insinuates a source of uplifting nutrients different than deep mixing. Chl *a* bloom is intimately dependent on nutrients supply, which in turn, in areas like the oligotrophic northern Red Sea [*Weikert*, 1987; *Labiosa et al.*, 2003; *Acker et al.*, 2008; *Raitsos et al.*, 2013] is mostly regulated by deep mixing or upwelling events.

The overall picture suggests that additional factors, acting synergistically with the heat loss from the sea surface, have generated the exceptional low SST observed in 2012 winter over the northernmost part of the
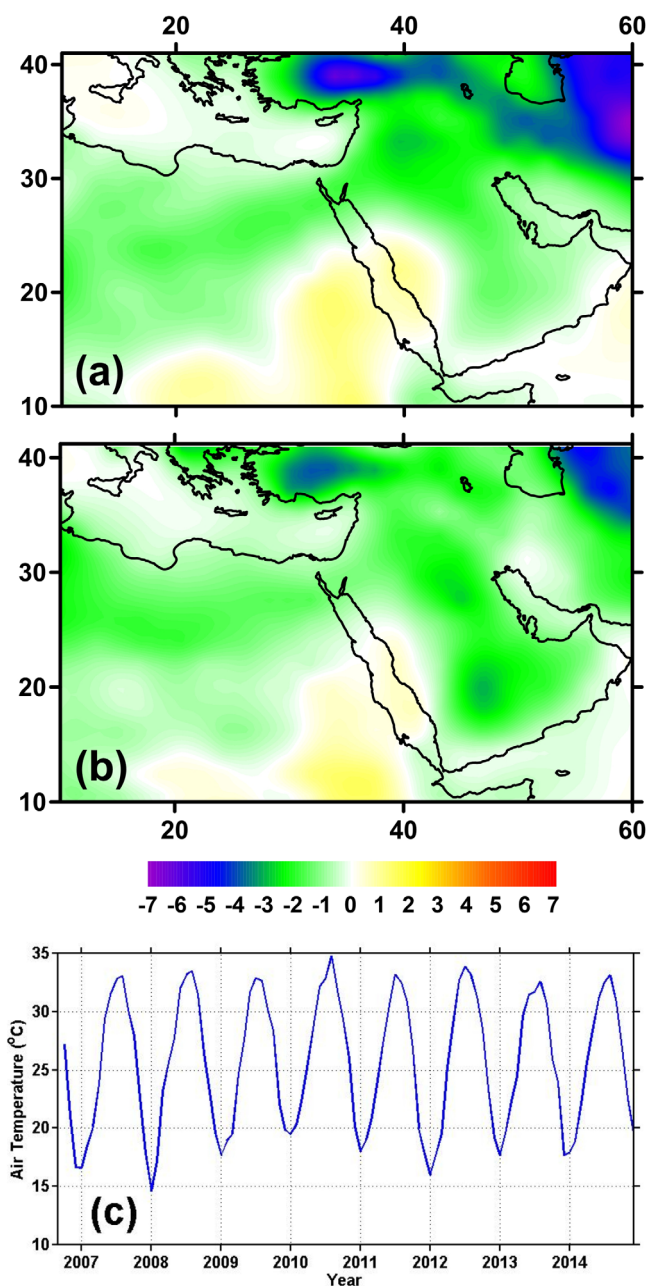
Figure 7. Mean winter (DJF) air temperature anomaly (°C) for (a) 2008 and (b) 2012 and (c) monthly mean air temperature from Eilat meteo station.

Red Sea. For example, lower than average SST during autumn and early winter generates a favorable precondition in producing cold events. In that case, a typical surface heat loss during winter can generate disproportional low SST. Factors propitious to create a preconditioning like the above include reduced air-sea heat flux prior to the forthcoming winter, blocking of warm water advection from the southern Red Sea, persistent upwelling events, and anomalous exchanges with the adjacent gulfs. The unusual high Chl *a* concentration observed in 2012 suggests that the occurrence of a persistent upwelling prior and during the winter of 2012 should be explored.

5. The Role of the Cyclonic Gyre

The Red Sea surface circulation includes several cyclonic and anticyclonic gyres, some of them to be year-round features. A cyclonic gyre prevailing over the northern Red Sea centered between 26°N and 27°N has been documented by several observational and modeling studies [*Morcos*, 1970; *Morcos and Soliman*, 1974; *Mallard*, 1974; *Clifford et al.*, 1997; *Eshel and Naik*, 1997; *Sofianos and Johns*, 2003, 2007; *Triantafyllou et al.*, 2014; *Zhan et al.*, 2014]. The significance of this cyclonic gyre, in terms of a water pump that uplifts subsurface water, has been already marked. According to *Sofianos and Johns* [2003], the gyre circulation favors intermediate water convection and about two thirds of RSOW is predicted to be produced in this cyclonic gyre during winter under strong buoyancy forcing. Occasional strengthening of the gyre gives rise to upwelling events like the ones clearly featured by SSH and SST data shown in the gyre snapshots of Figure 8. Moreover, gyre-related upwelling should be an occasional provider of nutrients transferred to the oligotrophic surface layers from nutrient-rich deeper layers [*Williams*, 2011].

To explore the gyre's temporal variability and its conditional role in regulating the SST over the northern Red Sea, we constructed an upwelling-proxy time series based on MODIS SST. This proxy is based on the difference of the SST between each of the two potential outer flanks of the gyre and its central part as depicted in Figure 9a. Upwelling is considered when both differences are positive (outer temperature greater than inner temperature). Time series for the upwelling proxy is presented in Figure 9b. Upwelling is very active before and during some winters with the lowest SST, like the ones in 2007 and especially in 2012. We investigate the
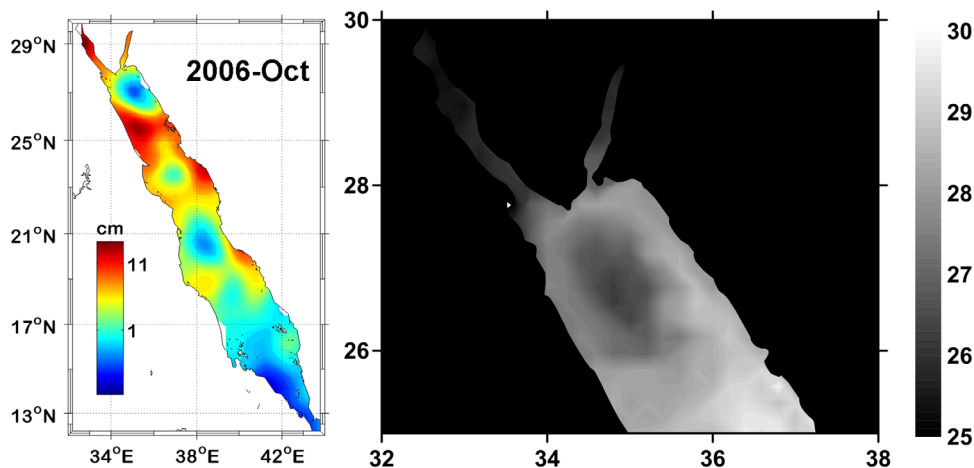
Figure 8. Indicative snapshots of the cyclonic gyre over the northernmost part of the Red Sea in October 2006 as derived by (left) monthly mean AVISO sea surface height and (right) weekly MODIS SST.

potential effect of the gyre on winter SST over the northern Red Sea analyzing two cases with different characteristics.

In terms of atmospheric forcing (expressed by Q_{net}), winters of 2007 and 2009 are similar (Figure 6c). In spite of this similarity, SST is lower during winter of 2007 (Figure 6a). In addition, surface waters are richer in Chl *a* in the winter of 2007 in comparison with 2009. Figure 9b shows that upwelling events are more often and stronger during autumn and December of 2006 than the same period in 2008. This indicates a more active cyclonic gyre just before the arrival of the winter in 2007 than in 2009. Indeed, the 6 month (July–December) mean SSH-induced circulation is clearly stronger in 2006 than in 2008 (Figure 10, top). The long-lasting gyre activity lifts subsurface colder and richer in nutrients water. This precondition results finally in lower SST and higher Chl *a* concentration in 2007 than 2009 under similar atmospheric forcing.
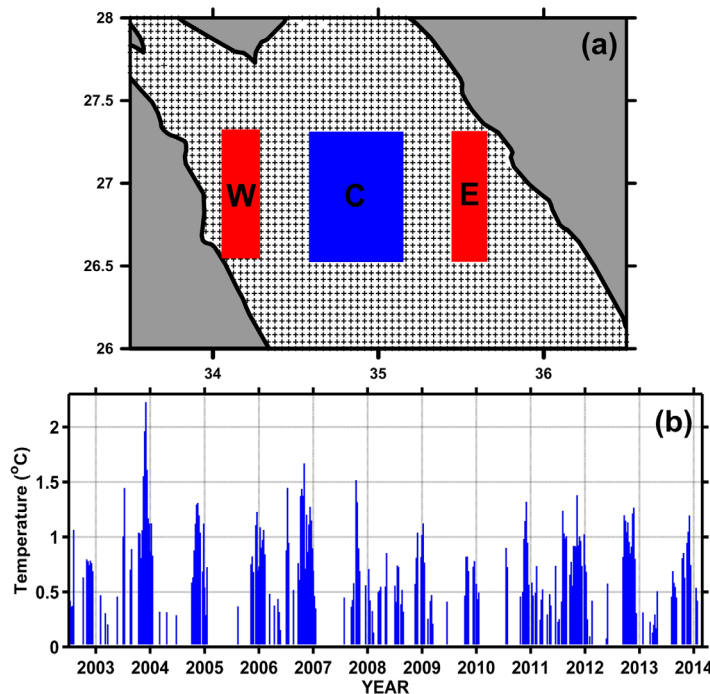

Figure 9. (a) The MODIS grid and the locations (W: western part, C: central, and E: eastern) over which spatially averaged SST were taken to check upwelling events; (b) upwelling events expressed as the mean of W-C and E-C when both are positive.

The comparison between the winters of 2010 and 2012 is more characteristic. Cyclonic gyre is very active almost throughout 2011, and similarly to 2006, uplifts to the surface colder water and creates a long-term negative SST anomaly over the northern Red Sea. From the years considered here, 2011 exhibits the most persistent upwelling event as inferred by the proxy time series. On the arrival of 2012 winter, surface layers over the northern Red Sea are colder than usual due to preexisting long-term upwelling. Though it is a mildly cold winter, it finally produces the lowest observed SST in the last 12 years. At the same time, persistent functioning of the cyclonic gyre provides significant amount of nutrients to the oligotrophic northern Red Sea.
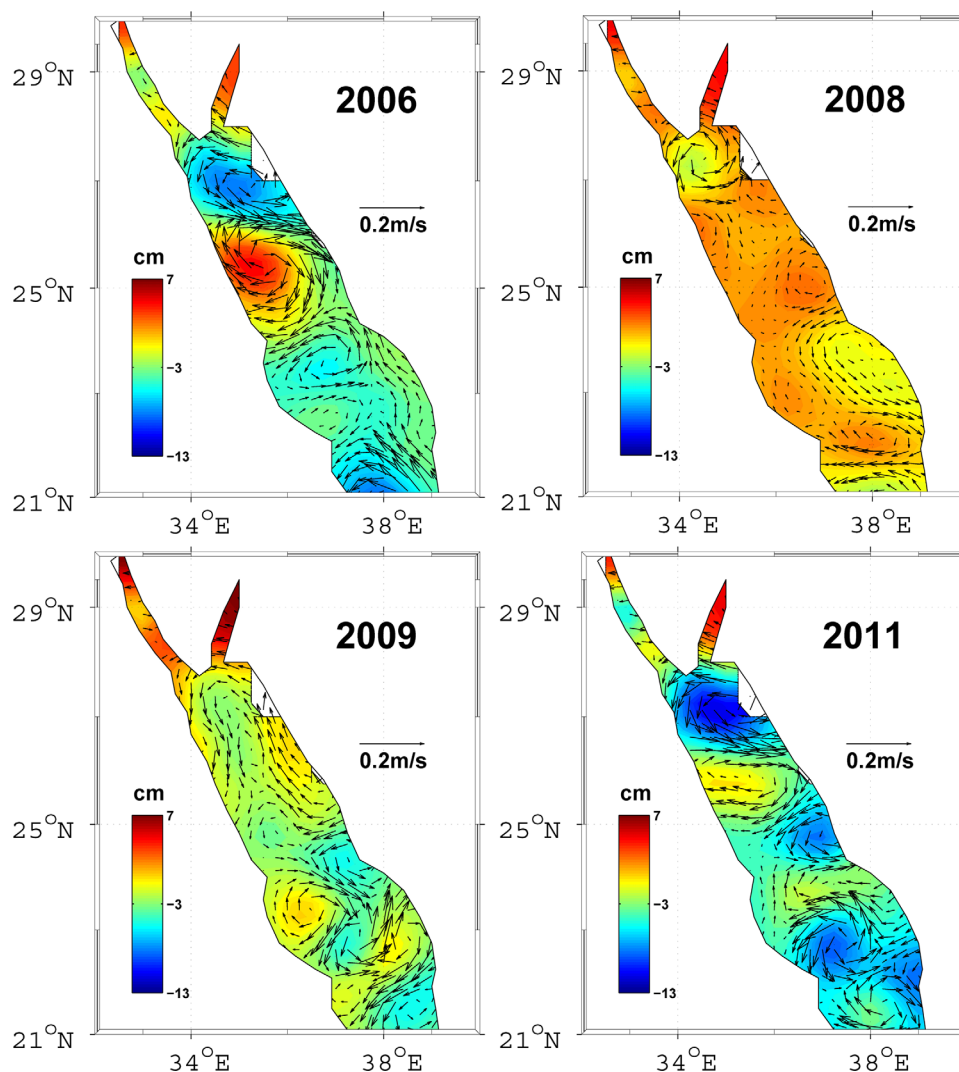
Figure 10. Six month mean (July–December) of sea surface height (SSH) and the SSH-induced sea surface circulation for (top left) 2006, (top right) 2008, (bottom left) 2009, and (bottom right) 2011.

Consequently, the winter of 2012 is associated with exceptionally high Chl *a* concentration. On the contrary, during the second half of 2009, prior to the warmest 2010 winter, the proxy shows weak gyre activity which in combination with weak atmospheric forcing results in the warmest winter SST of the 12 years. In addition, the low gyre activity suspends the nutrient supply from the deeper layers, which is reflected in the lowest Chl *a* concentration observed in 2010 winter. The dissimilar gyre activity in the second halves of 2009 and 2011 is obvious in SSH-induced circulation (Figure 10, bottom).

6. Concluding Remarks

The near-bottom water renewal in the Red Sea is a vital process and an eminent climatic signal for the basin. The exact origin and the formation mechanism of the near-bottom water in the Red Sea are practically unexplored. However, a series of studies analyzing data obtained during sparse oceanographic cruises or evaluating model outputs show that the very deep water of the Red Sea originates from the northernmost part of the basin, mostly from the Gulfs of Aqaba and Suez. The investigation of 12 year 4 km resolution MODIS SST and the findings of several hydrographic surveys suggest that formation of near-bottom water is a robust feature of the Red Sea overturning circulation. The amount of newly formed deep water is primarily a function of the intensity of the surface heat loss and shows considerable interannual variability.
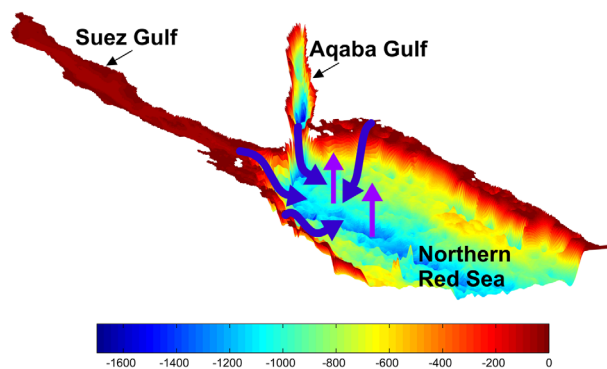
Figure 11. Bathymetry of the northern Red Sea and schematic representation of the deep water formation (blue paths). The vertical vectors indicate the water uplift induced by the cyclonic gyre functioning.

Suez and Aqaba Gulfs are the regular sources of the Red Sea near-bottom water. However, parts of coastal areas over the far north of the basin may also contribute, though occasionally. This water is dense enough to sink following the lateral slope path reaching the bottom layers. A schematic representation of the deep water renewal in the northern Red Sea is depicted in Figure 11.

Apart from the atmospheric fluxes, the interannual variability of deep water formation is also affected by the general oceanic circulation of the northern Red Sea. Analysis of satellite SST observations shows that persistent upwelling over the northern part of the basin occurring before and during winter leads to lower than normal SST. This sets a favorable precondition for intermediate and deep water formation even under winter conditions that cannot be characterized as extreme. The main expression of upwelling over the northernmost part of the Red Sea is the intermittent cyclonic gyre centered around 26°N–27°N. The strengthening (weakening) of the gyre can amplify (moderate) the winter surface cooling. At the same time, the gyre behavior significantly influences the phytoplankton bloom intensity that typically occurs in late February to early March in the open northern Red Sea. When the gyre is persistent, it raises adequate amounts of nutrients from the deeper layers leading to higher than usual Chl a concentrations. Changes in phytoplankton, the base of the marine food chain, influence every trophic level (including fish), and, in particular, may have profound repercussions for the functioning of coral reefs, and consequently for society.

Our study suggests that the cyclonic gyre over the northern Red Sea modulates the SST, which in turn regulates the intermediate and deep water formation process. Therefore, a future study devoted to the potential factors controlling the temporal variability of the gyre will be of particular interest. At the same time, further investigation is required to elucidate several aspects of the deep water formation in the Red Sea. The annual volume of the newly formed deep water entering the open sea from each of the Gulfs of Aqaba and Suez along with the role of the atmospheric forcing is matters that remain unclear. Our results highlight the importance of a multidisciplinary research effort aiming at a detailed description of the mechanism that renews the near-bottom water and sustains the ventilation of the deepest Red Sea ecosystem.

References

Abualnaja, Y., V. P. Papadopoulos, S. A. Josey, I. Hoteit, H. Kontoyiannis, and D. E. Raitsos (2015), Impacts of climate modes on air–sea heat exchange in the Red Sea, *J. Clim.*, *28*, 2665–2681, doi:10.1175/JCLI-D-14-00379.1.

Acker, J., G. Leptoukh, S. Shen, T. Zhu, and S. Kempler (2008), Remotely-sensed chlorophyll-a observations of the northern Red Sea indicate seasonal variability and influence of coastal reefs, *J. Mar. Syst.*, *69*, 191–204, doi:10.1016/j.jmarsys.2005.12.006.

Barbini, R., F. Colao, L. De Dominicis, R. Fantoni, L. Fiorani, A. Palucci, and E. S. Artamonov (2004), Analysis of simultaneous chlorophyll measurements by lidar fluorosensor, MODIS and SeaWiFS, *Int. J. Remote Sens.*, *25*(11), 2095–2110.

Biton, E., and H. Gildor (2011a), The coupling between exchange flux through a strait and dynamics in a small convectively driven marginal sea: The Gulf of Aqaba (Gulf of Eilat), *J. Geophys. Res.*, *116*, C06017, doi:10.1029/2011JC006944.

Biton, E., and H. Gildor (2011b), Stepwise seasonal restratification and the evolution of salinity minimum in the Gulf of Aqaba (Gulf of Eilat), *J. Geophys. Res.*, *116*, C08022, doi:10.1029/2011JC007106.

Brewin, R. J., D. E. Raitsos, Y. Pradhan, and I. Hoteit (2013), Comparison of chlorophyll in the Red Sea derived from MODIS-Aqua and in vivo fluorescence, *Remote Sens. Environ.*, *136*, 218–224, doi:10.1016/j.rse.2013.04.018.

Carpenter, J. H. (1965), The accuracy of the Winkler method for the dissolved oxygen analysis, *Limnol. Oceanogr.*, *10*, 135–140, doi:10.4319/ lo.1965.10.1.0135.

Cember, R. P. (1988), On the sources, formation, and circulation of the Red Sea deep water, *J. Geophys. Res.*, *93*, 8175–8191, doi:10.1029/ JC093iC07p08175.

Churchill, J. H., A. S. Bower, D. C. McCorkle, and Y. Abualnaja (2014), The transport of nutrient-rich Indian Ocean water through the Red Sea and into coastal reef systems, *J. Mar. Res.*, *72*, 165–181, doi:10.1357/002224014814901994.

Clifford, M., C. Horton, J. Schmitz, and L. H. Kantha (1997), An oceanographic nowcast/forecast system for the Red Sea, *J. Geophys. Res.*, *102*, 25,101–25,122, doi:10.1029/97JC01919.

Dee, D. P., et al. (2011), The ERA-Interim reanalysis: Configuration and performance of the data assimilation system, *Q. J. R. Meteorol. Soc.*, *137*, 553–597, doi:10.1002/qj.828.

Ducet, N., P. Y. Le Traon, and G. Reverdin (2000), Global high resolution mapping of ocean circulation from the combination of T/P and ERS-1/2, *J. Geophys. Res.*, *105*, 19,477–19,498, doi:10.1029/2000JC900063.

Eshel, G., and N. Naik (1997), Climatological coastal jet collision, intermediate water formation, and the general circulation of the Red Sea, *J. Phys. Oceanogr.*, *27*, 1233–1257, doi:10.1175/1520-0485(1997)027 < 1233:CCJCIW>2.0.CO;2.

Eshel, G., M. A. Cane, and M. B. Blumenthal (1994), Modes of subsurface, intermediate and deep water renewal in the Red Sea, *J. Geophys. Res.*, *99*, 15,941–15,952, doi:10.1029/94JC01131.

Feldman, G. C., and C. R. McClain (2012), Ocean Color Web, MODIS Reprocessing R2009, http://oceancolor.gsfc.nasa.gov, NASA Goddard Space Flight Cent.

Johns, W. E., and S. Sofianos (2012), Atmospherically forced exchange through the Bab el Mandeb Strait, *J. Phys. Oceanogr.*, *42*, 1143–1157, doi:10.1175/JPO-D-11-0157.1.

Labiosa, R. G., K. R. Arigo, A. Genin, S. G. Monismith, and G. Dijken (2003), The interplay between upwelling and deep convective mixing in determining the seasonal phytoplankton dynamics in the gulf of Aqaba: Evidence from SeaWiFS and MODIS. *Limnol. Oceanogr.*, *48*, 2355–2368, doi:10.4319/lo.2003.48.6.2355.

Mallard, C. (1974), Formation d'eau profonde en Mer Rouge, in *La Formation des Eaux Oceaniques Profondes*, pp. 115–125, Cent. Natl. de la Rech. Sci., Paris.

Mallard, C., and G. Soliman (1986), Hydrography of the Red Sea and exchanges with the Indian Ocean in summer, *Oceanol. Acta*, *9*(3), 249–269.

Manasrah, R., M. Badran, H. U. Lass, and W. Fennel (2004), Circulation and winter deep-water formation in the northern Red Sea, *Oceanologia*, *46*(1), 5–23.

Matt, S., and W. E. Johns (2007), Transport and entrainment in the Red Sea Outflow plume, *J. Phys. Oceanogr.*, *37*, 819–836, doi:10.1175/JPO2993.1.

Morcos, S., and G. F. Soliman (1974), Circulation and deep water formation in the Northern Red Sea in winter (based on R/V Mabahiss sections, January – February, 1935), in *L'oceanographie Physique de la Mer Rouge*, pp. 91–103, Cent. Natl. pour l'Exploitation des Océans, Paris.

Morcos, S. A. (1970), Physical and chemical oceanography of the Red Sea, *Oceanogr. Mar. Biol. Annu. Rev.*, *8*, 73–202.

Morel, A., and B. Gentili (2009), The dissolved yellow substance and the shades of blue in the Mediterranean Sea, *Biogeosciences*, *6*, 2625–2636, doi:10.5194/bg-6-2625-2009.

Murray, S., A. Hecht, and A. Babcock (1984), On the mean flow in the Tiran Strait in winter, *J. Mar. Res.*, *42*, 265–284, doi:10.1357/002224084788502738.

Murray, S. P., and W. Johns (1997), Direct observations of seasonal exchange through the Bab el Mandeb strait, *Geophys. Res. Lett.*, *24*, 2557–2560, doi:10.1029/97GL02741.

Paldor, N., and D. A. Anati (1979), Seasonal variations of temperature and salinity in the Gulf of Elat (Aqaba), *Deep Sea Res., Part A*, *26*(6), 661–672, doi:10.1016/0198-0149(79)90039-6.

Papadopoulos, V. P., Y. Abualnaja, S. A. Josey, A. Bower, D. E. Raitsos, H. Kontoyiannis, and I. Hoteit (2013), Atmospheric forcing of the winter air-sea heat fluxes over the northern Red Sea, *J. Clim.*, *26*, 1685–1701, doi:10.1175/JCLI-D-12-00267.1.

Plähn, O., B. Baschek, T. H. Badewien, M. Walter, and M. Rhein (2002), Importance of the Gulf of Aqaba for the formation of bottom water in the Red Sea, *J. Geophys. Res.*, *107*, 3108, doi:10.1029/2000JC000342.

Quadfasel, D., and H. Baudner (1993), Gyre-scale circulation cells in the Red Sea, *Oceanol. Acta*, *16*(3), 221–229.

Racault, M.-F., D. E. Raitsos, M. L. Berumen, R. Brewin, T. Platt, S. Sathyendranath, and I. Hoteit (2015), Phytoplankton phenology indices and their significance for Red Sea coral reef ecosystems, *Remote Sens. Environ.*, *160*, 222–234, doi:10.1016/j.rse.2015.01.019.

Raitsos, D. E., I. Hoteit, P. K. Prihartato, T. Chronis, G. Triantafyllou, and Y. Abualnaja (2011), Abrupt warming of the Red Sea, *Geophys. Res. Lett.*, *38*, L14601, doi:10.1029/2011GL047984.

Raitsos, D. E., Y. Pradhan, R. J. W. Brewin, G. Stenchikov, and I. Hoteit (2013), Remote sensing the phytoplankton seasonal succession of the Red Sea, *PLoS ONE*, *8*(6), e64909, doi:10.1371/journal.pone.0064909.

Raitsos, D. E., X. Yi, T. Platt, M.-F. Racault, R. J. W. Brewin, Y. Pradhan, V. P. Papadopoulos, S. Sathyendranath, and I. Hoteit (2015), Monsoon oscillations regulate fertility of the Red Sea, *Geophys. Res. Lett.*, *42*, 855–862, doi:10.1002/2014GL062882.

Rienecker, M. M., et al. (2011), MERRA: NASA's modern-era retrospective analysis for research and applications, *J. Clim.*, *24*, 3624–3648, doi: 10.1175/JCLI-D-11-00015.1.

Sofianos, S. S., and W. E. Johns (2003), An Oceanic General Circulation Model (OGCM) investigation of the Red Sea circulation: 2. Three-dimensional circulation in the Red Sea, *J. Geophys. Res.*, *108*(C3), 3066, doi:10.1029/2001JC001185.

Sofianos, S. S., and W. E. Johns (2007), Observations of the summer Red Sea circulation, *J. Geophys. Res.*, *112*, C06025, doi:10.1029/2006JC003886.

Sofianos, S. S., and W. E. Johns (2015), Water-mass formation, overturning circulation and the exchange of the Red Sea with the adjacent basins, in *Red Sea: the Formation, Morphology, Oceanography and Environment of a Young Ocean Basin*, edited by N. Rasul and I.C.F. Stewart, pp. 343–353. Springer-Verlag, Berlin Heidelberg.

Triantafyllou, G., F. Yao, G. Petihakis, K. P. Tsiaras, D. E. Raitsos, and I. Hoteit (2014), Exploring the Red Sea seasonal ecosystem functioning using a three dimensional biophysical model, *J. Geophys. Res.*, *119*, 1791–1811, doi:10.1002/2013JC009641.

Weikert, H. (1987), Plankton and the pelagic environment, in *Key Environments: Red Sea*, edited by A. J. Edwards and S. M. Head, pp. 90–111, Pergamon, Oxford, U. K.

Williams, R. G. (2011), Ocean eddies and plankton blooms, *Nat. Geosci.*, *4*, 739–740, doi:10.1038/ngeo1307.

Woelk, S., and D. Quadfasel (1996), Renewal of deep water in the Red Sea during 1982–1987, *J. Geophys. Res.*, *101*, 18,155–18,165, doi: 10.1029/96JC01148.

Wyrtki, K. (1974), On the deep circulation of the Red Sea, in *L'oceanographie Physique de la Mer Rouge*, pp. 135–163, Cent. Natl. pour l'Exploitation des Océans, Paris.

Yao, F., I. Hoteit, L. J. Pratt, A. S. Bower, P. Zhai, A. Köhl, and G. Gopalakrishnan (2014a), Seasonal overturning circulation in the Red Sea: 1. Model validation and summer circulation, *J. Geophys. Res. Oceans*, *119*, 2238–2262, doi:10.1002/2013JC009004.

Yao, F., I. Hoteit, L. J. Pratt, A. S. Bower, A. Köhl, G. Gopalakrishnan, and D. Rivas (2014b), Seasonal overturning circulation in the Red Sea: 2. Winter circulation, *J. Geophys. Res. Oceans*, *119*, 2263–2289, doi:10.1002/2013JC009331

Yu, L., X. Jin, and R. A. Weller (2008), Multidecade Global Flux Datasets from the Objectively Analyzed Air-sea Fluxes (OAFlux) Project: Latent and sensible heat fluxes, ocean evaporation, and related surface meteorological variables, *OAFlux Proj. Tech. Rep. OA-2008-01*, 64 pp., Woods Hole Oceanogr. Inst., Woods Hole, Mass.

Zhan, P., A. C. Subramanian, F. Yao, and I. Hoteit (2014), Eddies in the Red Sea: A statistical and dynamical study, *J. Geophys. Res. Oceans*, *119*, 3909–3925, doi:10.1002/2013JC009563.